Time dependent quantum simulations of two-qubit gates based on donor states in silicon

2006 J. Phys.: Condens. Matter 18 S767

(http://iopscience.iop.org/0953-8984/18/21/S04)

INSTITUTE OF PHYSICS PUBLISHING JOURNAL OF PHYSICS: CONDENSED MATTER

J. Phys.: Condens. Matter **18** (2006) S767–S776 doi:10.1088/0953-8984/18/21/S04

Time dependent quantum simulations of two-qubit gates based on donor states in silicon

A Kerridge[1], S Savory[2], A H Harker[1] and A M Stoneham[1]

[1] Department of Physics and Astronomy, University College London, Gower Street, London WC1E 6BT, UK
[2] Optical Networks Group, Department of Electronic and Electrical Engineering, University College London, Torrington Place, London WC1E 7JE, UK

E-mail: a.kerridge@ucl.ac.uk

Received 1 November 2005, in final form 22 December 2005
Published 12 May 2006
Online at stacks.iop.org/JPhysCM/18/S767

Abstract

Many quantum gate proposals make physical assumptions to ease analysis. Here we explicitly consider the effect of these assumptions for a particular two-qubit gate proposal, a cube-root-of-unity gate, in which the two qubits are donors in a semiconductor coupled via an intermediate 'control' spin. Our approach considers directly the electronic structures of the qubit and control impurity systems. We find that such gates are highly sensitive to environmental factors overlooked in analytically soluble models, but that there are regimes in which simplifying assumptions are valid and lead to high fidelity gates.

1. Introduction: quantum computation

The successful implementation of any quantum computer is dependent on the realization of quantum logic gates that manipulate quantum bits, or qubits. There are a diversity of proposals for potential quantum computers, including the adaptation of NMR techniques [1, 2], ion traps [3, 4], and a variety of solid-state devices [5, 6]. Here we consider one solid-state proposal [7] in which the qubits are defined by a pair of electron spins. In this proposal, the quantum entanglement required for any useful quantum computation is achieved by an effective coupling of the two-qubit spins via their mutual interaction with a third, 'control' spin. In this way, geometries can be conceived whereby there is no significant coupling in the ground state of such a system (i.e. the qubit spins are effectively isolated), but in an excited state there is sufficient overlap of the one-electron states to allow a controlled manipulation of the qubit spins. An analytical model for a gate of this type has been given [8], where it has also been shown that a variety of universal quantum gates can be constructed in this way. In this paper, we consider a more physical model of this type of gate and study how the properties of such a gate are affected by small interactions that were neglected in the previous treatment. Section 2 presents an idealized analytical model of the cube-root-of-unity (CRU) gate, and shows that

the controlled NOT (CNOT) gate can be constructed from it, demonstrating its universality in conjunction with one-qubit operations. Section 3 describes the quantum mechanical model of the qubit–control system, with an explicit discussion of the electronic structure of the control donor and of the donors embodying the qubits. This model is applied in section 4 to practical considerations in the operation of the gate.

2. The cube-root-of-unity gate

2.1. An analytical model

The CRU gate may be formed from two qubits, which we label A and B, and a control bit, C. Following [8] we define our basis as

$$\mathbf{b} = \begin{bmatrix} \mathbf{v}_\mathrm{g} \\ \mathbf{v}_\mathrm{e} \end{bmatrix} \tag{1}$$

with

$$\mathbf{v}_\mathrm{s} = \psi_\mathrm{A}\psi_\mathrm{B}\psi_\mathrm{C}^\mathrm{s}\,[|000\rangle, |001\rangle, |010\rangle, |011\rangle, |100\rangle, |101\rangle, |110\rangle, |111\rangle]^\mathrm{T}, \tag{2}$$

where $|i_\mathrm{A} j_\mathrm{B} k_\mathrm{C}\rangle$ defines the spin components of the wavefunction, with $|0\rangle$ corresponding to a spin up state, and $|1\rangle$ to a spin down state. The spatial component of the wavefunction is assumed to be independent of the spin state, and the excited state to be considered is an optical excitation of the electron with spatial wavefunction ψ_C, hence the additional label. An effective Hamiltonian can be defined in terms of exchange couplings between the spins, allowing the time dependence of this Hamiltonian [8] to be studied analytically. This analysis reveals that the behaviour of the system can be defined in terms of two integers M and N that relate the operation time of a quantum gate to the magnitude of the exchange couplings and Zeeman energies of the spins. In the absence of an applied magnetic field the analysis simplifies, and the gate proposed here can be defined in terms of a single integer N.

The free propagation of the system between laser pulses can be written in terms of the unitary operator

$$\mathbf{U} = \begin{bmatrix} \mathbf{U}^\mathrm{g} & 0 \\ 0 & \mathbf{U}^\mathrm{e} \end{bmatrix} \tag{3}$$

where $\mathbf{U}^\mathrm{g}$ and $\mathbf{U}^\mathrm{e}$ are 8×8 matrices, given in terms of the Hamiltonians $\mathbf{H}$ of the ground and excited states by

$$\mathbf{U}^\mathrm{s} = \exp[-\mathrm{i}\mathbf{H}^\mathrm{s} t]. \tag{4}$$

The ground state is assumed to be one in which there is no coupling of the electrons (i.e. $\mathbf{H}^\mathrm{g}$ is diagonal) and, furthermore, there is assumed to be no coupling of the two qubit spins in the excited state. This leaves only the coupling of each qubit spin to the control spin. In practice, the only off-diagonal terms which are non-zero in this approximation are those which couple states $|1\rangle$ to $|2\rangle$, $|1\rangle$ to $|4\rangle$, $|6\rangle$ to $|3\rangle$, and $|6\rangle$ to $|5\rangle$, where we have replaced the binary notation with its decimal equivalent ($|001\rangle = |1\rangle$, $|010\rangle = |2\rangle$, etc). We assume a perfectly symmetric system, with the qubits equally spaced either side of the control and in identical environments, so that the strengths of their couplings to the control are identical and given by $2J_\mathrm{C}$. It is evident that for this system the energies of states $|2\rangle$ and $|4\rangle$ are identical, a fact which allows $\mathbf{U}^\mathrm{e}$ to be written in closed form (see [8] for details).

We require that the control bit C is disentangled from the qubits at the end of the gate operation, and this is ensured by imposing one further condition, namely that the time between pulses is given by

$$J_\mathrm{C} t = \frac{n\pi}{3}, \tag{5}$$

where n is an integer. Upon a permutation of the basis to $[|0\rangle, |2\rangle, |4\rangle, |6\rangle, |1\rangle, |3\rangle, |5\rangle, |7\rangle]^{\mathrm{T}}$, we can express $\mathbf{U}^{\mathrm{e}}$ as

$$\mathbf{U}^{\mathrm{e}} = \begin{bmatrix} \mathbf{U}^{+} & 0 \\ 0 & \mathbf{U}^{-} \end{bmatrix}, \tag{6}$$

where $\mathbf{U}^{\pm}$ defines the propagation for all states with control spin up/down. $\mathbf{U}^{+}$ is given by

$$\mathbf{U}^{+} = \begin{bmatrix} \exp\left[-\mathrm{i}\frac{2\pi}{3}\right] & 0 & 0 & 0 \\ 0 & \frac{1}{2}\exp\left[-\mathrm{i}\frac{\pi}{3}\right] & \frac{\sqrt{3}}{2}\exp\left[-\mathrm{i}\frac{5\pi}{3}\right] & 0 \\ 0 & \frac{\sqrt{3}}{2}\exp\left[-\mathrm{i}\frac{5\pi}{3}\right] & \frac{1}{2}\exp\left[-\mathrm{i}\frac{\pi}{3}\right] & 0 \\ 0 & 0 & 0 & \exp\left[-\mathrm{i}\frac{2\pi}{3}\right] \end{bmatrix} \tag{7}$$

and similarly for $\mathbf{U}^{-}$. It can be seen here that the effect of the coupling of each qubit spin to the control is to mix states $|2\rangle$ and $|4\rangle$, in a manner similar to that which would be observed if the two spins were coupled directly. The CRU gate has the property that three applications of it to a given three-spin system return the system to its initial state. For the remainder of this paper, and with no loss of generality, we only consider the evolution of systems initially with control spin up, i.e. $\mathbf{U}_{\mathrm{CRU}} = \mathbf{U}^{+}$. Our calculations, however, do allow for the entangling of the control spin, and we shall consider this in section 4.

2.2. *Characterization of the CRU gate*

We can characterize the entangling properties of the CRU gate in terms of the local invariants G_1 and G_2 [9]. These local invariants uniquely characterize those properties of a gate that are not modifiable by local transformations. Defining $\mathbf{Q}$ and $\mathbf{U}_{\mathrm{B}}$ as

$$\mathbf{Q} = \frac{1}{\sqrt{2}} \begin{bmatrix} 1 & 0 & 0 & \mathrm{i} \\ 0 & \mathrm{i} & 1 & 0 \\ 0 & \mathrm{i} & -1 & 0 \\ 1 & 0 & 0 & -\mathrm{i} \end{bmatrix}, \tag{8}$$

$$\mathbf{U}_{\mathrm{B}} = \mathbf{Q}^{\dagger}\mathbf{U}\mathbf{Q}, \tag{9}$$

then, with $\mathbf{m} = \mathbf{U}_{\mathrm{B}}^{\mathrm{T}}\mathbf{U}_{\mathrm{B}}$, G_1 and G_2 are given by

$$G_1 = \frac{\mathrm{tr}^2(\mathbf{m})}{16\det\mathbf{U}}, \tag{10a}$$

$$G_2 = \frac{\mathrm{tr}^2(\mathbf{m}) - \mathrm{tr}(\mathbf{m}^2)}{4\det\mathbf{U}}. \tag{10b}$$

In principle, G_1 and G_2 can be used to reconstruct the eigenspectrum of $\mathbf{m}$. For $\mathbf{U}_{\mathrm{CRU}}$ we obtain $G_1^{\mathrm{CRU}} = (-13 + \mathrm{i}3\sqrt{3})/32$, $G_2^{\mathrm{CRU}} = -3/2$. For any local operation $G_1 = 1$ and $G_2 = 3$, and so we immediately see that the CRU gate is a non-local gate, allowing the entanglement of the qubit spins. The values of the local invariants of the CRU gate also allow us to identify this gate with others with the same local properties.

We also define one further parameter, $\Delta(\mathbf{U})$, related to the entanglement fidelity $F(\mathbf{U})$ [10] by $\Delta = 1 - F(\mathbf{U})$ with

$$F(\mathbf{U}) = |\mathrm{tr}(\mathbf{U}_{\mathrm{CRU}}^{\dagger}\mathbf{U})|^2/16. \tag{11}$$

Here $\mathbf{U}$ is a calculated gate, and $\Delta(\mathbf{U}) \approx 0$ for gates close to $\mathbf{U}_{\mathrm{CRU}}$.

2.3. Universality of the CRU gate

It has been shown (see, for example, [11]) that the CNOT gate in conjunction with one-qubit operations is universal. Here we show that the CNOT gate can be constructed from the CRU gate (more details are given in the appendix), and hence the CRU gate together with one-qubit operations is universal. We first define an arbitrary single-qubit gate

$$\mathbf{U}_1(\alpha, \beta, \gamma, \delta) = \mathbf{R}_z(\alpha)\mathbf{R}_y(\beta)\mathbf{R}_z(\gamma)\exp[\mathrm{i}\delta], \tag{12}$$

where

$$\mathbf{R}_i(\theta) = \exp\left[-\mathrm{i}\frac{\theta}{2}\boldsymbol{\sigma}_i\right], \tag{13}$$

and $\boldsymbol{\sigma}_i$ is a Pauli spin matrix. We form

$$\mathbf{U}_{\mathrm{int}} = \mathbf{U}_{\mathrm{CRU}} \cdot [\mathbf{I}_2 \otimes \mathbf{R}_z(\pi)] \cdot \mathbf{U}_{\mathrm{CRU}}, \tag{14}$$

where $\mathbf{I}_2$ is the 2×2 identity matrix, and note that $\mathbf{U}_{\mathrm{int}}$ is diagonal. We then construct the matrix $\mathbf{U}_{\mathrm{int}} \cdot \mathbf{U}_1 \cdot \mathbf{U}_{\mathrm{int}}$ and evaluate the local invariants G_1 and G_2. These are given by

$$G_1 = \tfrac{1}{16}(3\cos(\beta) - 1)^2, \tag{15a}$$

$$G_2 = \tfrac{9}{8}(1 + \cos^2(\beta)) - \tfrac{3}{4}\cos(\beta). \tag{15b}$$

The local invariants of the CNOT gate are $G_1 = 0$ and $G_2 = 1$, conditions which are satisfied for $\beta = \arccos(\frac{1}{3})$. Therefore the gate

$$\mathbf{U}_{\mathrm{CNOT}_l} = \mathbf{U}_{\mathrm{int}} \cdot \left[\mathbf{I}_2 \otimes \mathbf{R}_y\left(\arccos\left(\tfrac{1}{3}\right)\right)\right] \cdot \mathbf{U}_{\mathrm{int}} \tag{16}$$

is locally equivalent to the CNOT gate, and so the universality of the CRU gate with one-qubit operations is demonstrated. The CNOT gate is related to this gate by

$$\mathbf{U}_{\mathrm{CNOT}} = \mathbf{k}_1 \cdot \mathbf{U}_{\mathrm{CNOT}_l} \cdot \mathbf{k}_2, \tag{17}$$

where $\mathbf{k}_1$ and $\mathbf{k}_2$ are local transformations. Examples of such transformations that satisfy equation (17) are given in the appendix.

3. The model system

We take as our model system shallow donor states in silicon, for which effective mass theory (EMT) is well suited both for isolated impurities [12, 13] and for 'molecular' species [14, 15]. In its most basic form, EMT shows that a shallow donor state in a medium of dielectric constant ε_{r} can be considered to be a product of a hydrogenic envelope, and an oscillating Bloch-like function. If the envelope function is 'smooth' in comparison to the oscillating term, then to a good approximation the oscillating term can be ignored. Then the defect states are given by solutions to the hydrogenic Hamiltonian, given in atomic units by

$$\hat{H}_{\mathrm{EMT}} = -\frac{\nabla^2}{2m^*} - \frac{1}{\varepsilon_{\mathrm{r}} r}. \tag{18}$$

In more sophisticated formulations of the theory, 'central cell' corrections, which consider the local electronic structure of the defect, are included to give more realistic energies and wavefunctions. Here we present results of using a single-parameter model potential which approximately incorporates this correction in a form that lends itself to straightforward evaluation of Hamiltonian matrix elements. This model potential is fitted to give good agreement with experimental data for phosphorus, arsenic, antimony, and bismuth donor energies in silicon when used in scaled Hartree–Fock (HF) calculations, in which the standard HF equations are solved, but with m replaced by m^* and r^{-1} by this model potential. Note

Table 1. Experimental and calculated energies in meV of donor states in Si. All experimental data are taken from [20]. An asterisk indicates that experimental value was not available, and so approximate values were taken from [21].

	HEMT	P ($\sigma = 0.2343$)		As ($\sigma = 0.2067$)		Sb ($\sigma = 0.2669$)		Bi ($\sigma = 0.1739$)	
	Calc.	Exp.	Calc.	Exp.	Calc.	Exp.	Calc.	Exp.	Calc.
1s	−31.40	−45.59	−43.82	−53.76	−49.80	−42.74	−39.86	−70.98	−69.37
2s	−7.84	−10.6*	−8.70	−9.11	−9.13	−9.4*	−8.35	−8.78	−10.64
$2p_0$	—	−11.48	—	−11.50	—	−11.51	—	−11.44	—
$2p_\pm$	—	−6.40	—	−6.40	—	−6.28	—	−6.37	—
2p	−7.85	−8.09	−7.85	−8.10	−7.85	−8.06	−7.85	−8.05	−7.85

that while we include this correction, we neglect properties particular to silicon, namely its anisotropic effective mass, and its sixfold-degenerate conduction band minima. The effects of these properties have been considered elsewhere [16–18]. We have not estimated the overlap factors associated with the Bloch functions; these will give a factor that varies rapidly from one site to another, but the key analysis will not be affected [13, 19].

3.1. The model potential

We take as our model potential, which replaces the $(\varepsilon_r r)^{-1}$ term of equation (18),

$$V(r) = \frac{1}{\varepsilon_r r}\left[1 + (\varepsilon_r - 1)\exp[-\sigma r]\right], \tag{19}$$

and note that

$$\lim_{r\to 0} V(r) = \frac{1}{r} \tag{20a}$$

$$\lim_{r\to \infty} V(r) = \frac{1}{\varepsilon_r r}, \tag{20b}$$

as would be expected for a central cell correction. Table 1 shows the results of using this model potential in scaled HF calculations for isolated donors in silicon, in addition to the hydrogenic effective mass (HEMT) results obtained by the solution of equation (18). Here we take $m^* = 0.3$ a.u., and $\varepsilon_r = 11.4$. Note that since we are ignoring the anisotropy of the effective mass, we do not obtain distinct $p_\pm$ and p_0 states, and so we take a weighted average of the energies of these states, $E_p = (2E_{p_\pm} + E_{p_0})/3$, to compare to our calculated values. The energies calculated here were obtained using a contracted Gaussian basis of seven primitives per function, chosen to balance accuracy with efficiency in later calculations.

As can be seen, the model potential gives good agreement with experiment, i.e. a significant lowering of the 1s state with significant electron density near $r = 0$, and little or no effect on states such as 2s and 2p which have much lower amplitudes in this region. Figure 1 shows the 1s states for each of the donors. For each state the electron density is enhanced near $r = 0$ due to the potential, but the 'tails' of the states are similar, as one might expect. We note that an effect of these corrected states is a significant reduction in the donor–donor exchange couplings, with an order of magnitude difference between the HEMT and Bi donor couplings. As a result the variation of exchange coupling with separation is very different from that assumed in [8].

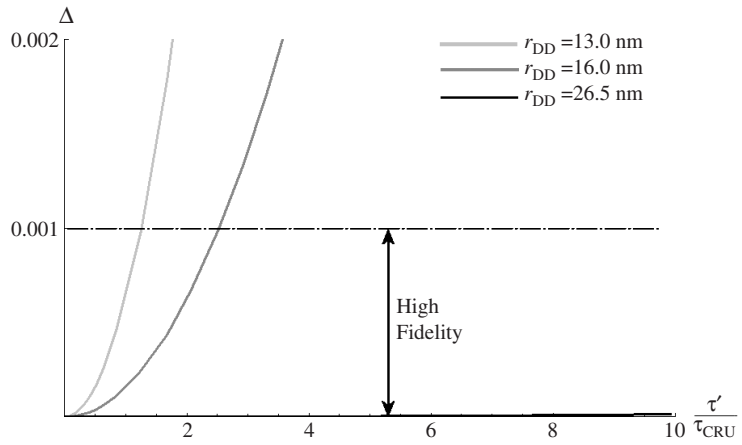

Figure 1. Variation of Δ, the deviation from perfect fidelity, with time for a selection of CRU gates with different donor–donor separations. Note that the curve for the largest separation is barely distinguishable from the horizontal axis.

4. 'Realistic' gate simulations

For our more realistic gates, we take our donor states to be Bi 1s states, and our control states to be the ground and first optically excitable states of a deeper effective mass donor, with the ground state energy of ∼150 meV. Note that although we obtain these isolated states via scaled HF equations, there is currently no SCF cycle within our time dependent calculations. In keeping with [8] we only consider the evolution of the spin states, and so in this sense our simulations should be viewed as a time dependent configuration interaction calculation, with the contributing configurations defined in terms of their spin components. Each configuration has an identical spatial component, with the only degree of freedom being the choice as to whether the control electron is in its ground or excited state. This in turn means that there is some degree of non-orthogonality in our one-electron states, most notable at small control–qubit separations.

There are four different extensions to the idealized model presented in section 2 which we can consider. These are:

(i) donor–donor coupling during gate operation;
(ii) evolution of the ground state;
(iii) asymmetry in the system;
(iv) error in the interpulse time.

4.1. Donor–donor coupling during gate operation

We characterize the effect of this coupling in terms of the parameters G_1, G_2, and Δ, as defined in section 2. With the inclusion of donor–donor coupling, we obtain off-diagonal terms in the Hamiltonian connecting states $|2\rangle\&\ |4\rangle$ and $|3\rangle\&\ |5\rangle$, with this coupling given by $2J_Q$. Then J_Q and J_C can be defined in terms of the total energies of the various spin states:

$$J_C = \tfrac{1}{4}(E_1 - E_0) = \tfrac{1}{4}(E_6 - E_0), \tag{21a}$$

$$J_Q = \tfrac{1}{2}(E_2 - E_0 - 2J_C). \tag{21b}$$

Table 2. A comparison of the ideal CRU gate with simulated gates that include donor–donor coupling. Gate operation times are calculated using only J_C.

r_{DD} (nm)	J_C (GHz)	J_Q (GHz)	τ_{CRU} (ps)	δ_G	Δ
4.0	437	322	0.762	2.98	0.749
5.0	565	97.0	0.590	1.45	0.0936
6.5	671	37.4	0.496	0.594	0.0101
7.5	750	16.6	0.443	0.246	1.60×10^{-3}
8.5	803	7.37	0.415	0.104	2.74×10^{-4}
10.5	829	4.85	0.403	0.0134	4.50×10^{-6}
12.0	803	0.161	0.416	2.30×10^{-3}	1.33×10^{-7}
18.5	472	0.0730	0.706	1.77×10^{-3}	7.82×10^{-8}
26.5	157	4.73×10^{-3}	2.12	3.38×10^{-4}	2.44×10^{-9}

Since we are considering the effect of neglecting J_Q on the gate operation, we calculate our gate operation time solely on the basis of our value of J_C. At large separations, for which $|J_C| \gg |J_Q|$, we would expect this to have little effect on the gate, but these calculations will allow us to put a lower bound on donor–donor separations for high fidelity gate operation. Here we consider high fidelity gates to be those for which $\Delta < 10^{-3}$, and measure the error in G_1 and G_2 using $\delta_G = \sqrt{\delta_1^2 + \delta_2^2}$ with $\delta_1 = |G_1^{CRU} - G_1|$ and similarly for δ_2. The results of our simulations can be seen in table 2. These results show that a minimum donor–donor separation of $\sim$8 nm is required to satisfy our criterion for a high fidelity gate, but for separations greater than this, much higher fidelities are quickly achieved. This, of course, tells us nothing about how the system evolves over longer timescales, only that over the gate operation time there is a regime in which high fidelity gates can be constructed. The evolution of the system over longer timescales will be considered in the following section.

4.2. Ground state evolution

Since any useful quantum algorithm will require a series of gate operations, we must consider how the system evolves for time periods significantly longer than the gate operation time. Here we study the system evolution over a period of $10\tau_{CRU}$ after a gate operation has been performed for a series of donor–donor separations. In the ground state, the qubit spins couple to the ground state of the control spin in addition to each other, and since this coupling will be stronger than the donor–donor coupling, it is expected that this will put further constraints on high fidelity gates. Figure 1 shows the variation of Δ with time for several system geometries.

As can be seen, there is a rapid increase in Δ even for high fidelity gates after only a few τ_{CRU}, suggesting that the minimum donor–donor separation for a useful gate is $r_{DD} \geqslant 13$ nm, a stronger constraint than that imposed by G_1, G_2, and Δ alone.

4.3. Asymmetry in the system

In this section we consider the effects of more realistic system geometries, moving away from the symmetric model proposed in section 2. It should be noted that the parameters of the gate were optimized for a symmetric geometry, and there may be methods for improving the fidelity for asymmetric systems over that which we present here. We consider three systems with fixed r_{AC}, and set $r_{BC} = r_{AC} + r'$, with r' varying over the range $\pm 10\%$ r_{AC}. This results in asymmetric coupling of the qubit spins to the control, and so we define our gate operation time in terms of J_{AC}. Figure 2 shows the results of these calculations. We find that our simulated

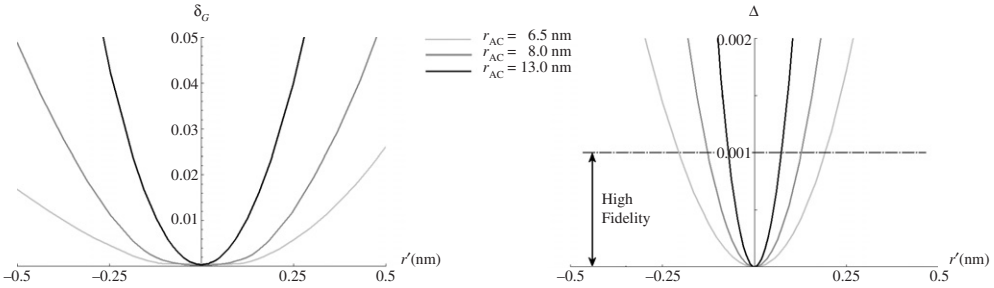

Figure 2. Local invariant error, δ_G, and deviation from perfect fidelity, Δ, for several asymmetric geometries.

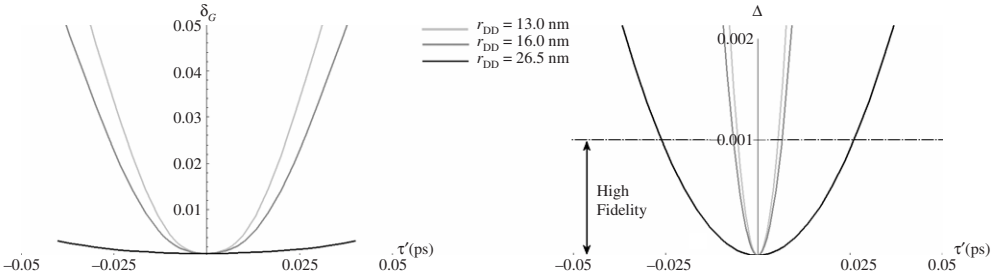

Figure 3. Errors in δ_G and Δ induced by errors in the interpulse duration.

gates are extremely sensitive to asymmetry, with the maximum error allowed to maintain high fidelity being a single nearest neighbour spacing ($r' = 0.235$ nm). We note that this effect is most significant for large donor–donor separations.

4.4. Inaccuracies in gate operation time

Finally, we consider the effect of errors in gate operation time. For the CRU gate, we have $J_C\tau$ = constant, and so the errors introduced here could be attributed to either inaccuracies in the duration between excitation and de-excitation laser pulses or in the evaluation of the exchange coupling itself. Figure 3 shows the results of variation in τ over a range ± 0.05 ps, for three symmetric systems: as shown in table 2, we expect the gate times to range from about 0.4 to 2 ps or more at large separations.

As can be seen, the gates with larger qubit–qubit separation are less sensitive to this error. This is to be expected, since the absolute error in operation time corresponds to a smaller *relative* error for larger qubit separations. Again, a high sensitivity of the systems to this variation is observed, and this highlights the need for an accurate configuration process for any future quantum processor based on this technology, a process that would identify exchange couplings of qubit pairs to high accuracy.

5. Conclusions

We have shown that a universal quantum gate can be modelled using time dependent quantum simulation methods. Under certain conditions, these simulated gates compare well to an idealized analytical model of such a gate, but are highly sensitive to deviations from this

idealized model due to interactions and inaccuracies present in a real physical system. We have quantified the errors introduced by the inclusion of these terms, and this should be viewed as a base on which to consider more sophisticated gates that are more robust against such environmental factors. In particular, we highlight the need for a highly accurate configuration procedure that would need to be applied to any high fidelity quantum processor constructed using this technology.

Acknowledgments

We are grateful to Dr P T Greenland for valuable discussions. We would like to thank EPSRC for financial support from a Basic Technology grant.

Appendix

Taking equation (7) as our starting point, we form $\mathbf{U}_{\rm int} = \mathbf{U}_{\rm CRU} \cdot [\mathbf{I}_2 \otimes \mathbf{R}_z(\pi)] \cdot \mathbf{U}_{\rm CRU}$ given by

$$\mathbf{U}_{\rm int} = \begin{bmatrix} \exp\left[\mathrm{i}\frac{\pi}{6}\right] & 0 & 0 & 0 \\ 0 & \exp\left[-\mathrm{i}\frac{\pi}{6}\right] & 0 & 0 \\ 0 & 0 & \exp\left[\mathrm{i}\frac{5\pi}{6}\right] & 0 \\ 0 & 0 & 0 & \exp\left[-\mathrm{i}\frac{5\pi}{6}\right] \end{bmatrix} \tag{22}$$

and note that $\mathbf{U}_{\rm int}$ remains diagonal when acted upon by $\mathbf{I}_2 \otimes \mathbf{R}_z(\theta)$, and in particular that $\mathbf{U}_{\rm int} \cdot \mathbf{I}_2 \otimes \mathbf{R}_z(\theta) = \mathbf{I}_2 \otimes \mathbf{R}_z(\theta) \cdot \mathbf{U}_{\rm int}$. We then form $\mathbf{U}_{\rm int} \cdot \mathbf{I}_2 \otimes \mathbf{U}_1 \cdot \mathbf{U}_{\rm int}$, where $\mathbf{U}_1$ is an arbitrary one-qubit gate (equation (12)). We require $\mathbf{U}_{\rm int} \cdot \mathbf{I}_2 \otimes \mathbf{U}_1 \cdot \mathbf{U}_{\rm int}$ to be locally equivalent to the CNOT gate, represented by the unitary operator

$$\mathbf{U}_{\rm CNOT} = \begin{bmatrix} 1 & 0 & 0 & 0 \\ 0 & 1 & 0 & 0 \\ 0 & 0 & 0 & 1 \\ 0 & 0 & 1 & 0 \end{bmatrix}. \tag{23}$$

In order to achieve this we require the two operators to have identical local invariants G_1 and G_2 as specified by equations (10*a*) and (10*b*). $\mathbf{U}_{\rm int} \cdot \mathbf{I}_2 \otimes \mathbf{U}_1 \cdot \mathbf{U}_{\rm int}$ can be written as

$$\begin{aligned} \mathbf{U}_{\rm int} \cdot \mathbf{I}_2 \otimes \mathbf{U}_1 \cdot \mathbf{U}_{\rm int} &= \exp[\mathrm{i}\delta]\mathbf{U}_{\rm int} \cdot (\mathbf{I}_2 \otimes \mathbf{R}_z(\alpha))(\mathbf{I}_2 \otimes \mathbf{R}_y(\beta))(\mathbf{I}_2 \otimes \mathbf{R}_z(\gamma)) \cdot \mathbf{U}_{\rm int} \\ &= \exp[\mathrm{i}\delta](\mathbf{I}_2 \otimes \mathbf{R}_z(\alpha)) \cdot \mathbf{U}_{\rm int} \cdot (\mathbf{I}_2 \otimes \mathbf{R}_y(\beta)) \cdot \mathbf{U}_{\rm int} \cdot (\mathbf{I}_2 \otimes \mathbf{R}_z(\gamma)), \end{aligned} \tag{24}$$

and so, since $\mathbf{I}_2 \otimes \mathbf{R}_z(\theta)$ is a local operation, the local invariants of $\mathbf{U}_{\rm int} \cdot \mathbf{I}_2 \otimes \mathbf{U}_1 \cdot \mathbf{U}_{\rm int}$ are independent of α, γ, and δ. Choosing $\alpha = \gamma = \delta = 0$ with $\beta = \arccos(\frac{1}{3})$ gives a gate locally equivalent to the CNOT gate. This gate is specified by

$$\begin{aligned} \mathbf{U}_{\rm CNOT_\prime} &= \mathbf{U}_{\rm int} \cdot \left[\mathbf{I}_2 \otimes \mathbf{R}_y\left(\arccos\left(\tfrac{1}{3}\right)\right)\right] \cdot \mathbf{U}_{\rm int} \\ &= \begin{bmatrix} \sqrt{\frac{2}{3}}\exp\left[\mathrm{i}\frac{\pi}{3}\right] & -\frac{1}{\sqrt{3}} & 0 & 0 \\ \frac{1}{\sqrt{3}} & \sqrt{\frac{2}{3}}\exp\left[-\mathrm{i}\frac{\pi}{3}\right] & 0 & 0 \\ 0 & 0 & \sqrt{\frac{2}{3}}\exp\left[-\mathrm{i}\frac{\pi}{3}\right] & -\frac{1}{\sqrt{3}} \\ 0 & 0 & \frac{1}{\sqrt{3}} & \sqrt{\frac{2}{3}}\exp\left[\mathrm{i}\frac{\pi}{3}\right] \end{bmatrix}. \end{aligned} \tag{25}$$

This gate can be made identical to the CNOT gate by applying local transformations, i.e.

$$\mathbf{U}_{\rm CNOT} = \mathbf{k}_1 \cdot \mathbf{U}_{\rm CNOT_\prime} \cdot \mathbf{k}_2, \tag{17}$$

As an example, local transformations that satisfy equation (17) are given by

$$\mathbf{k}_1 = \exp\left[\mathrm{i}\frac{\pi}{4}\right]\mathbf{R}_z\left(\frac{\pi}{2}\right)\otimes\left(\mathbf{R}_y\left(\frac{\pi}{2}\right)\cdot\mathbf{R}_z\left(\frac{-\pi}{2}\right)\cdot\mathbf{R}_y(-\arctan[\sqrt{2}])\right)$$
$$= \frac{1}{2}\begin{bmatrix} (1+\mathrm{i})\exp[-\mathrm{i}a] & (-1+\mathrm{i})\exp[-\mathrm{i}a] & 0 & 0 \\ (1+\mathrm{i})\exp[\mathrm{i}a] & (1-\mathrm{i})\exp[\mathrm{i}a] & 0 & 0 \\ 0 & 0 & (-1+\mathrm{i})\exp[-\mathrm{i}a] & -(1+\mathrm{i})\exp[-\mathrm{i}a] \\ 0 & 0 & (-1+\mathrm{i})\exp[\mathrm{i}a] & (1+\mathrm{i})[\mathrm{i}a] \end{bmatrix}, \tag{26}$$

where $a = \frac{1}{2}\arctan[\sqrt{2}]$, and

$$\mathbf{k}_2 = \mathbf{I}_2 \otimes \left(\mathbf{R}_y\left(\arctan\left[\frac{1}{\sqrt{2}}\right]\right)\cdot\mathbf{R}_z(\pi)\right)$$
$$= -\mathrm{i}\begin{bmatrix} \cos[b] & \sin[b] & 0 & 0 \\ \sin[b] & -\cos[b] & 0 & 0 \\ 0 & 0 & \cos[b] & \sin[b] \\ 0 & 0 & \sin[b] & -\cos[b] \end{bmatrix}, \tag{27}$$

where $b = \frac{1}{2}\arctan\left[\frac{1}{\sqrt{2}}\right]$ and so the CNOT operation can be performed using four CRU operations and local transformations.

References

[1] Gershenfeld N A and Chuang I L 1997 *Science* **275** 30
[2] Chuang I L *et al* 1998 *Proc. R. Soc.* A **454** 447
[3] Cirac J I and Zoller P 1995 *Phys. Rev. Lett.* **74** 4091
[4] Steane A M 1997 *Appl. Phys.* B **64** 623
[5] Kane B E 1998 *Nature* **393** 133
[6] Loss D and DiVincenzo D P 1998 *Phys. Rev.* A **57** 120
[7] Stoneham A M, Fisher A J and Greenland P T 2003 *J. Phys.: Condens. Matter* **15** L447
[8] Rodriquez R *et al* 2004 *J. Phys.: Condens. Matter* **16** 2757
[9] Makhlin Yu 2002 *Quantum Inf. Process* **1** 243
[10] Fortunato E M *et al* 2002 *J. Chem. Phys.* **116** 7599
[11] Brylinski J L and Brylinski R 2002 *Mathematics of Quantum Computation* ed R Brylinski and G Chen (Boca Raton, FL: Chapman and Hall/CRC) p 101
[12] Kohn W L and Luttinger J M 1955 *Phys. Rev.* **98** 915
[13] Stoneham A M 1975 *Theory of Defects in Solids* (Oxford: Oxford University Press)
[14] Stoneham A M and Harker A H 1975 *J. Phys. C: Solid State Phys.* **8** 1102
[15] Stoneham A M and Harker A H 1975 *J. Phys. C: Solid State Phys.* **8** 1109
[16] Baldereschi A 1970 *Phys. Rev.* B **1** 4673
[17] Wellard C J *et al* 2003 *Phys. Rev.* B **68** 195209
[18] Ahn D 2005 *J. Appl. Phys.* **98** 033709
[19] Andres K *et al* 1981 *Phys. Rev.* B **24** 244
[20] Ramdas A K and Rodriguez S 1981 *Rep. Prog. Phys.* **44** 1297
[21] Kohn W and Luttinger J M 1955 *Phys. Rev.* **97** 1721